Research Journal of Physical Sciences ISSN 2320–4796
Vol. **1(6),** 17-23, July **(2013)** *Res. J. Physical Sci.*

Structural, Optical and Electrical Characteristics of Nanostructured ZnO Thin Films with various Thicknesses deposited by RF Magnetron Sputtering

G. Anil Kumar[1], M.V. Ramana Reddy[1] and Katta Narasimha Reddy[2]
[1]Department of Physics, Osmania University, Hyderabad, INDIA
[2]Department of Physics, Mahatma Gandhi University, Nalgonda AP, INDIA

Available online at: www.isca.in
Received 5th June 2013, revised 11th June 2013, accepted 31st June 2013

Abstract

Zinc oxide thin films having various thicknesses between 100 nm and 400 nm were deposited on glass substrates by RF magnetron sputtering technique. These films have been analyzed for their structural, optical and electrical properties as a function of the thickness by a series of characterization techniques, including X-ray diffraction (XRD), scanning electron microscopy (SEM), energy dispersive spectroscopy (EDS), resistivity measurements and spectrophotometer. The micro structural parameters, such as the lattice constant, crystallite size, stress and strain are calculated. All these films exhibited strong (002) diffraction peaks corresponding to hexagonal wurtzite structure. The visible range transmittance was found to be over 90%. The optical band gap increased from 3.21 eV to 3.37 eV and the electrical resistivity decreased from $5.21x10^{-2}$ Ω cm to $1.47x10^{-2}$ Ω cm with increase of film thickness.

Keywords: ZnO, RF magnetron sputtering, film thickness, optical transmittance and electrical resistivity.

Introduction

Zinc oxide (ZnO) is a wide band gap direct semiconductor having band gap of 3.37 eV at room temperature. It also possesses large exciton-binding energy of 60 meV. ZnO is an attractive semiconductor due to its low cost, nontoxicity, high stability and high transparency in the visible wavelength. It is a promising material for many applications in toxic gas sensors[1], solar cell windows[2], blue and ultraviolet (UV) light emitting devices[3], transparent conductors[4], surface acoustic devices[5], photovoltaic devices[6]**,** etc. In the recent past, a large variety of growth techniques, such as, RF magnetron sputtering[7], reactive thermal evaporation[8], spray pyrolysis[9]**,** chemical vapor deposition (CVD)[10], molecular beam epitaxy (MBE)[11]**,** pulsed laser deposition (PLD)[12], sol–gel process[13]**,** electro-deposition[14]**,** etc., have been used for the preparation of ZnO thin films. It was also experimentally found that the structural and optical properties of ZnO thin films are sensitive to the deposition conditions[15,16,17]. Among the above mentioned methods, radio frequency (rf) magnetron sputtering has been found to be more useful for uniform deposition over large area of substrate material. More over it is also useful in having good adhesion to the substrate, better reproducibility, high deposition rates and easy control of the composition of the films deposited using this technique. The properties of the RF magnetron sputter deposited films mainly depend on the various deposition parameters for example substrate temperature, partial pressure of oxygen, sputtering power, sputtering pressure in the chamber, substrate bias voltage and thickness of the film.

In the present investigation, an attempt has been made to produce highly textured zinc oxide nano thin films in the absence of oxygen gas environment on glass substrates using RF magnetron sputtering technique. The effect of thickness on the structural, optical and electrical properties has been investigated.

Material and Methods

ZnO thin film deposition: ZnO thin films in the present investigation were deposited on glass substrates using RF magnetron sputtering from a pure ZnO target material. The target used was having a diameter of 2 inch and thickness of 3 mm with 99.99% purity. The substrates were thoroughly cleaned using ultrasonic technique. The deposition equipment was an indigenous with circular planar magnetron sputtering system, it is composed of a vacuum chamber (residual gas pressure approximately 10^{-5} mbar) in which are faced a substrate holder and an r.f. magnetron cathode (5cm diameter), separated by approximately 7 cm. A power supply operated at a frequency of 13.56 MHz. The deposition chamber was pumped with rotary and turbo molecular pumps combination. The pressure in the chamber was measured using Pirani and Penning gauge combination. The magnetron target assembly was mounted on top of the sputter chamber such that the sputtering can be performed by sputter down configuration. Highly pure Ar gas was used as sputtering gas .The flow rate of argon gas was controlled by MKS mass flow controller. The deposition chamber was maintained with a vacuum of 5 x 10^{-5} mbar before introduction of the Argon gas in the chamber. The sputtering target was pre-sputtered for 15 min to remove any residual impurity on the surface of the target. The target was water-cooled and the substrate was kept at room temperature initially. During the deposition of the film, the substrate temperature was

maintained around 100^0C. The films were deposited with different thicknesses ranging from 100 nm to 400 nm as a function of deposition time by keeping the other deposition parameters such as argon partial pressure, substrate temperature, sputtering power and sputtering gas pressure as constant. The sputtering conditions maintained during the preparation of ZnO thin films are tabulated in table-1.

Table-1
Deposition parameters maintained during the deposition of ZnO films as a function of thickness

Sputtering target	ZnO (99.99%) 2-in. diameter and 3 mm thickness
Target to substrate distance	70 mm
Substrates	glass
Ar gas flow rate	80 sccm
Ultimate pressure	$5x10^{-5}$ mbar
Sputtering pressure	$1.2x10^{-2}$ mbar
Substrate temperature	373K
Sputtering power	50 W
Thickness	100nm - 400 nm

Characterization: The crystallinity of the films was investigated by x-ray diffraction measurement technique (Philips X'Pert X-Ray Diffractometer) in the 2θ range of 20°-80° using CuK_{α} radiation of wavelength λ=1.5406 Å at room temperature. X-ray tube was operated at a voltage of 40 kV and curret of 30 mA with scanning speed of 0.5 degree per minute. Optical transmittance spectra of films were recorded using a SHIMAZDU 3100 UV-Vis Spectrophotometer over wavelength range from 200 to 800 nm. The surface morphology was studied by scanning electron microscope (SEM) (model EVO 18 manufactured by Carl Zeiss), for which an EDS is attached (model INCA, X-act manufactured by Oxford Instruments) for estimating composition in the films. The electrical resistivity measurements were carried out using Keithley 2400 source meter with Pro4 probe from Lucas labs. SP4 probe head made up of tungsten carbide with 0.0016 inches tip radius, 1.58 mm tip spacing and 85 grams pressure was used for all the measurements. Measurements were made at 5 different places on each film and their average was taken as the sheet resistance of that film. Quartz crystal thickness monitor was used for the measurement of thickness of the deposited films.

Results and Discussion

Film thickness: Figure-1 indicates the variation of the thin film thickness with deposition time. It is found from the figure that the thickness increases linearly from 100 to 400 nm when the deposition time increases from 20 to 80 minutes.

Structural properties: Figure-2 shows XRD patterns of zinc oxide thin films with various thicknesses. All the XRD peaks in the figure correspond to the reflection of wurtzite-structured ZnO planes and all the samples have a strong (0 0 2) peak. This suggests that all the deposited ZnO thin films found to be hexagonal wurtzite structure and are preferentially oriented along the c-axis perpendicular to the substrate surface. The c-axis orientation in ZnO films can be understood by the model proposed by Drift[18]. According to Drift model, nucleation's with various orientations can be formed at the initial stage of the deposition of the film and each nucleus competes to grow but only nuclei having the fastest growth rate on the substrate can survive, i.e., c-axis orientation is achieved.

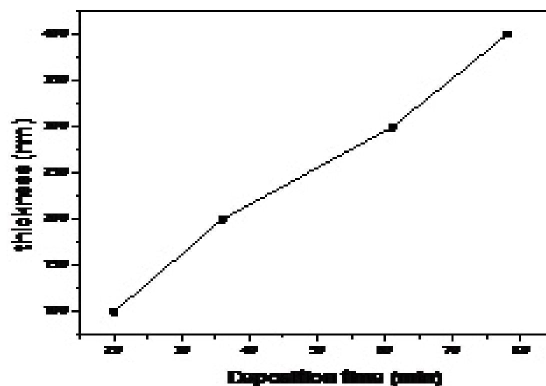

Figure-1
Variation of the film thickness with the deposition time

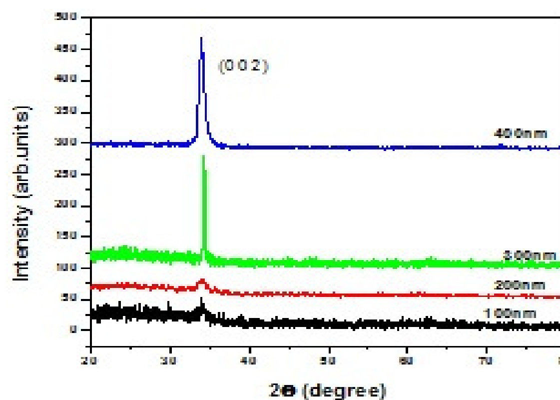

Figure-2
XRD patterns of ZnO films deposited at various thicknesses

With increasing the thickness of the film, the locations of the measured diffraction peaks do not change significantly but the intensities of the peaks become more pronounced and found to be sharper. This is due to the crystallinity of the films being improved and grain size becoming larger when elevating the film thickness. Similar behavior was reported by Assunc¸a˜o et al.[19]. As thickness of the film increases from 100 to 400 nm, the FWHM decreases from 0.57 to 0.14 and the crystallite sizes increases from 15 to 63 nm.

From the figure-2, it was also noted that the peak position corresponding to the ZnO (0 0 2) reflection for films with different

thickness is at lower 2Θ values as compared to (0 0 2) peak position of ZnO powder (34.43^0). This indicates that the films grown at different thicknesses are in a state of uniform compressive stress with tensile components parallel to the c-axis[20].

The average crystallite sizes of the films deposited at various thicknesses have been estimated using the following Scherrer's formula[21]

$$D = K\lambda/(\beta \cos \theta) \qquad (1)$$

Where K is the shape factor of a value having 0.94, λ is the wavelength of X-ray, β is full width at half maxima (FWHM) in radians and θ is the Bragg's diffraction angle.

The average uniform strain (e_{zz}) in the lattice along the c-axis in the randomly oriented ZnO films deposited on different thicknesses have been estimated from the lattice parameters using the following expression[22],

$$e_{zz}=(d-d_0)/d_0 \qquad (2)$$

Where ''d'' is the lattice parameter of the ZnO film calculated from (0 0 2) peak of XRD pattern and the "d_0'' is the lattice parameter for the bulk zinc oxide.

The elastic stress (σ) of the films can be determined from Hoffman's relation[23]:

$$\sigma = (2C_{13} - (C_{11}+C_{12}) C_{33}/C_{13}).e_{zz} \qquad (3)$$

Here C_{ij} are elastic stiffness constants (C_{11} = 2.1 x 10^{11} N/m^2 , C_{33} = 2.1x 10^{11}N/m^2, C_{12} = 1.2 x 10^{11} N/m^2, and C_{13} = 1.05 x10^{11} N/m^2). This yields the following numerical relation for the stress derived from the change in the lattice parameter (d).

$$\sigma\ (N\ m^{-2}) = -\ 4.5\times10^{11}.e_{zz} \qquad (4)$$

Dislocation density (δ) and number of crystallites per unit area (N) have been calculated using the crystallite size and thickness of the film[24-26].

$$\text{Dislocation density } (\delta) = 1/ D^2 \qquad (5)$$

$$\text{Number of crystallites per unit area } (N) = t/D^3 \qquad (6)$$

where "t" is the thickness of the ZnO thin film.

The various structural parameters for ZnO thin films deposited at different thicknesses were calculated and are represented in table-2.

The structural parameters such as the lattice parameter, grain size, stress, dislocation density, strain and number of grains per unit area are given in figures 3(a)-(f) respectively and correlated with thickness.

From the Figure-3 (a) it has been observed that with increase in thickness of the film the lattice constant found to be decreased. The change in lattice constant for the thin film deposited upon the substrate clearly suggests that the thin film's grains are under stress and it may be due to the change in the nature and concentration of the native imperfections. This may cause either elongation (tensile) or compression of the lattice parameters. The density of the film is, therefore, expected to change in accordance with the changes in the lattice constant.

Figure-3(b) shows that the film's crystallite size depends on thickness of the film. When the deposition process begins, there are many nucleation centers on the substrate and small crystallites are produced during the deposition process. Since the films are deposited only for a short period of time, the small crystallites on the substrate are not able to grow into large crystallites, and due to this the thinner films have smaller crystallites than the thicker films. With increasing deposition time, film thickness increases hence, the crystallinity of the films is improved and the crystallite sizes become larger.

The average internal stress for the zinc oxide thin films deposited at different thicknesses (Figure-3(c)) is found to be compressional in nature. The negative sign indicates that the films may be in a state of compressive stress. The total stress in the film commonly consists of two components. One is the intrinsic stress may be arise due to impurities, defects and lattice distortions in the crystal, and the other is the extrinsic stress arise due to the lattice mismatch and thermal expansion coefficient mismatch between the substrate and film. The extrinsic stress in thin films normally relaxes if the thickness of the film is larger[27]. In the present case, thickness of all the films is above 100 nm.

Table-2
Structural parameters of ZnO thin films deposited at different thicknesses

Thickness (nm)	Lattice parameter (nm)	Grain size (nm)	Dislocation density (10^{15} lines/m^2)	Number of grains/unit area(10^{16} m^{-2})	Strain (10^{-3})	Stress (GPa)
100	0.5255	15.2	4.32	2.84	9.21	-4.14
200	0.5242	27.5	1.32	0.961	6.72	-3.02
300	0.5223	42.0	0.566	0.404	3.07	-1.38
400	0.5213	63.1	0.251	0.159	1.15	-0.51

Thus, the extrinsic stress component may not be significant and predominantly intrinsic in nature. In the present case of RF magnetron sputtering process, this intrinsic stress arises due to the bombardment of the energetic particles. The films deposited at low temperature exhibits strong compressive stress. The thinner films exhibits strong compressive stress. In the RF sputtering, the highly energetic particles could be implanted below the ZnO surface, which is likely to induce high intrinsic stresses by creating the defects[28]. But for a ZnO thin film grown at high temperature, the strain quickly relaxed due to the high kinetic energy imparted to the particles[29]. The earlier investigations on zinc oxide films (Gupta and Mansingh[30]) also found the presence of stress in these films and it was attributed to oxygen interstitial defects. It is well known fact that the oxygen interstitials are less pronounced if the formation energy is more in ZnO films. In the present study all the depositions were carried out in oxygen deficient atmosphere. So the possibility of the formation of oxygen interstitials may be ruled out. In the present investigation for the growth of thin films, the formation of Zn interstitials and the oxygen vacancies are expected.

The micro strain (e) and the dislocation density (δ) are found to exhibit a slow decreasing trend (figure- 3(d) and figure- 3(e)). The decrease in e and δ at higher thicknesses may be due to the movement of interstitial Zn atoms from inside the crystallites to the grain boundary, which in turn leads to a reduction in the concentration of lattice imperfections. Further, the number of crystallites per unit area is found to decrease with increasing thickness of films (figure-3(f)).

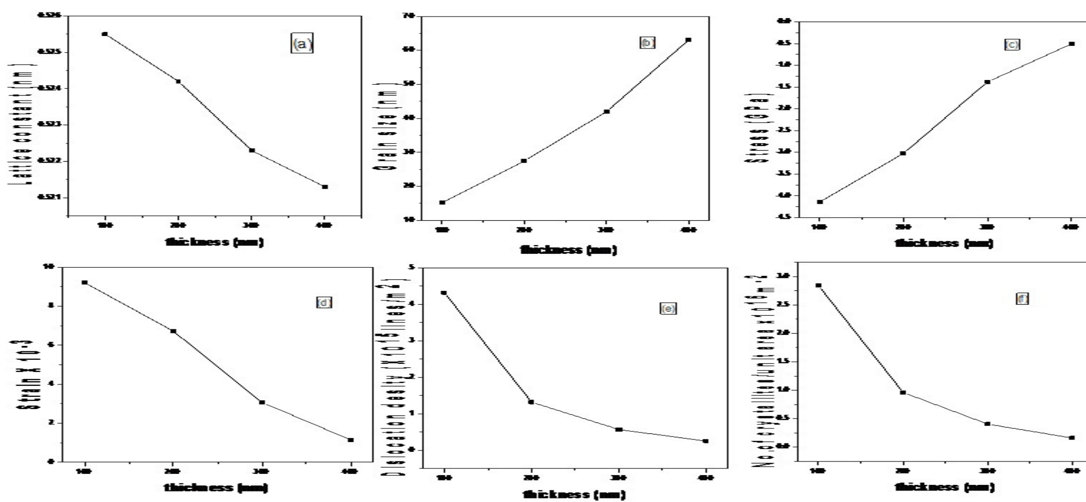

Figure-3
(a) Lattice constant, (b) grain size, (c) stress, (d) strain, (e) dislocation density and (f) number of crystallites as function of thickness of the film

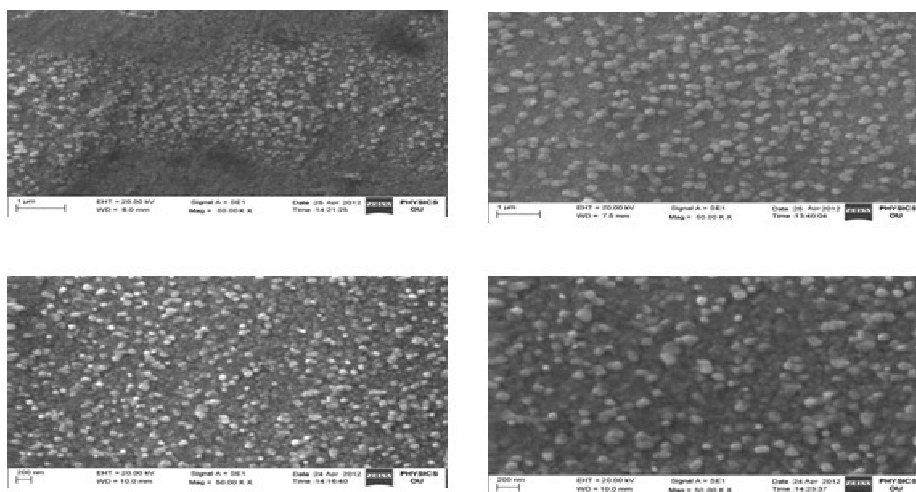

Figure-4
SEM images of the ZnO thin films as a function of thickness.
(a)100nm (b)200nm (c)300nm (d)400nm

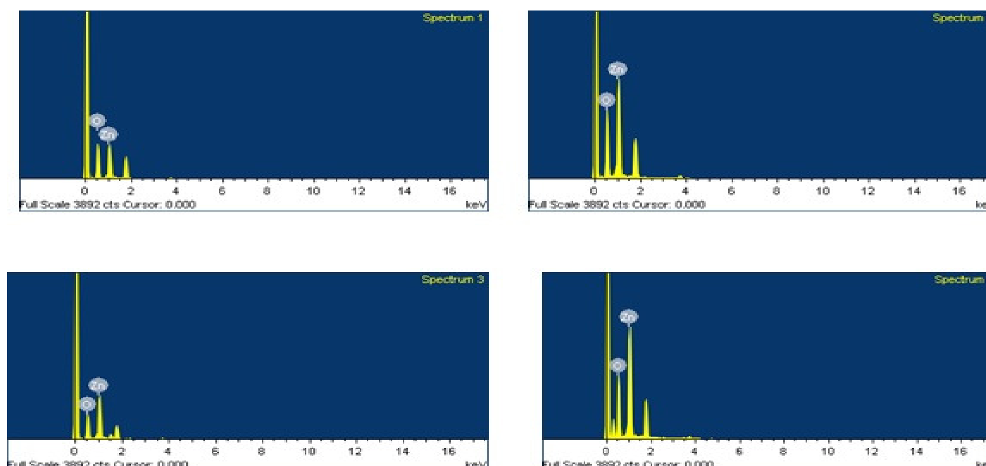

Figure-5
EDS spectra of the ZnO thin films as a function of thickness.
(a)100nm (b)200nm (c)300nm (d)400nm

Surface morphology: Figure-4 indicates the SEM images of the ZnO thin films as a function of thickness. The SEM images clearly indicate that the sputtered ZnO films were found to be uniform, homogenous, crack free surfaces. The irregular shaped grains were observed at the film thickness of 100 nm. The film deposited at the thickness of 200 nm shows a uniform grain distribution and grain size also found to be larger than 100 nm thick film. When the films deposited at higher thicknesses (300 nm and 400 nm) the grain size was progressively increased. The results are in good agreement with the XRD data.

The energy dispersive spectroscopy (EDS) was employed (figure-5) to identify the composition of the as deposited ZnO films at different thicknesses. It is observed from the above figure-5 that the films consists of zinc and oxygen (Table-3). It is clearly seen that the stoichiometry of the films depends on the thickness of the film. The films contained excess oxygen at the film thicknesses of 100 and 200 nm. The zinc content in the films increased with increase in thickness of the film. As the thickness of the film approached 300 nm, it was observed that zinc and oxygen ratio was found to be 1:1 and the films are nearly stoichiometric.

Table-3
Composition analysis of ZnO films at different thicknesses using EDS

Thickness (mn)	Element	Weight %	Atomic %	Zn / O ratio
100	O.K. Zn K	38.32 61.68	71.74 28.26	0.39
200	O.K. Zn K	25.27 74.73	59.02 40.98	0.69
300	O.K. Zn K	20.24 79.76	47.04 52.96	1.12
400	O.K. Zn K	23.76 76.24	53.35 46.65	0.87

Optical properties: Figure-6 shows the optical transmittance spectra of ZnO films as a function of thickness. All the films are showing optical transmittance of above 90% in visible range of wavelengths and appeared a sharp absorption edge near 380 nm. As the thickness increases from 100 nm to 400 nm, the transmittance of the films decreased to 10%. The low optical transmittance at higher film thickness can be predicted due to high surface light scattering of the films. The shift of absorption edge toward lower wavelength was observed with the increase of film thickness, this was due to widening of the band gap.

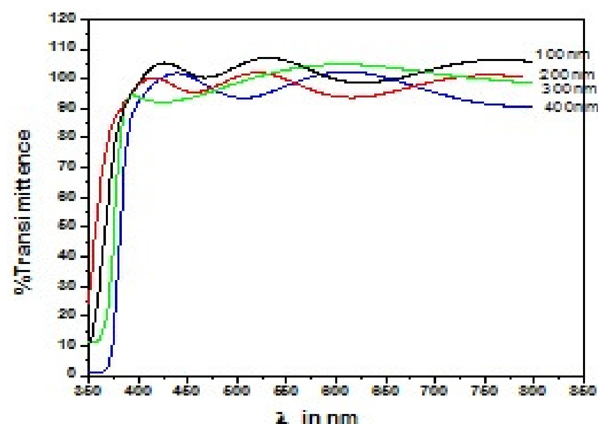

Figure-6
Variation of Optical transmittance with wavelenghth of ZnO films at various thicknesses

The optical band gap of zinc oxide thin films was calculated using the Tauc's method[31]. The optical absorption coefficient (α) was calculated using the relation

$$\alpha = -(1/t)\ln(T) \quad (7)$$

where "t" and "T" are the film thickness and transmittance respectively.

The optical band gap (Eg) of the film can be obtained by plotting $(\alpha h\nu)^2$ versus hν and extrapolating the straight line portion of this plot to the energy axis. Figure-5 is the plot of $(\alpha h\nu)^2$ versus hν. The linear dependence of $(\alpha h\nu)^2$ to hν indicates that ZnO films are exhibiting direct band transitions. The photon energy at the point where $(\alpha h\nu)^2$ is zero is optical band gap (Eg). From figure-7, Eg for the four films is 3.21, 3.25, 3.33 and 3.37 eV, respectively. It is clearly observed that with decrease of film thickness, the optical band gap (Eg) of the films was found to be increased. This means that the thickness of the film also affects the optical band gap (Eg) of the zinc oxide film.

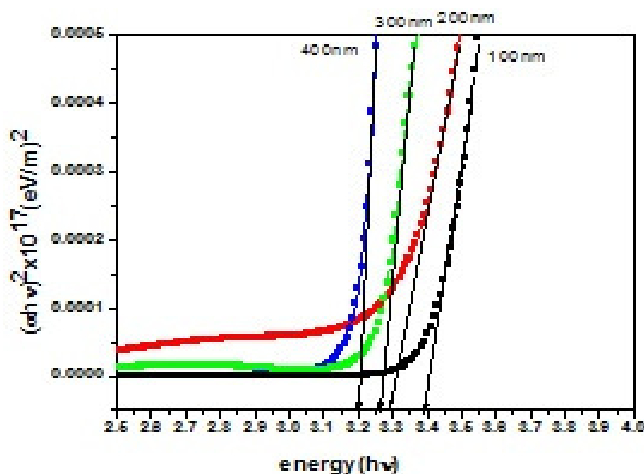

Figure-7
(αhν)2 versus hν plot for ZnO films at various thicknesses

Electrical properties: As thickness of the zinc oxide film increases from 100nm to 400nm, the electrical resistivity of the films decreased from 5.21 x 10^{-2} Ω cm to 1.47 x 10^{-2} Ω cm. In general, the electrical resistivity of the films is affected by three types of electron scattering mechanisms. They are isotropic background scattering (due to the combined effects of phonons and point defects), scattering due to the external surface, and scattering due to a distribution of planar potentials (grain boundaries)[32]. In this investigation, the variation of the electrical resistivity of the zinc oxide films with film thickness may be attributed to the grain boundary scattering.

Conclusion

ZnO thin films with various thicknesses were prepared by RF magnetron sputtering technique and the structural, optical and electrical properties were studied. The structural analysis showed that all the ZnO thin films were highly c-axis oriented. With the increase of film thickness, the crystalline quality of ZnO thin film was improved and the average internal stress developed in the films were compression in nature which was likely governed by a dominant recrystallization process. From optical transmittance spectra , it is found that all the films present a high optical transmittance of above 90% and the optical band gap reduces from 3.37 eV to 3.21 eV, with the increase of thickness of film i.e. optical band gap of semiconductor nanocrystals can be tuned as desired by varying thickness of the film. As film thickness increases from 100nm to 400nm, the electrical resistivity of the films decreased from 5.21 x 10^{-2} Ω cm to 1.47 x 10^{-2} Ω cm.

Acknowledgements

The authors thank the Head, Department of physics, Osmania University, Hyderabad for providing necessary experimental facilities [UGC-SAP (DSA-II)]. One of the authors (GAK) thanks UGC, New Delhi for awarding the SRF under the UGC scheme of RFSMS. One of us (MVRR) thanks OU-DST-PURSE Programme, Osmania University, Hyderabad and UGC New Delhi [UGC MRP file no.41-907/2012(SR)] for providing financial assistance to carry out this work.

References

1. Mitra A.P. and Chatterjee H.S. Maiti, ZnO thin film sensor, *Mater. Lett.* **35,** 33–38 **(1998)**
2. Jeong W.J., Kim S.K. and Park G.C., Preparation and characteristic of ZnO thin film for an application of solar cell, *Thin Solid Films* **180,** 506 **(2006)**
3. Bagall D.M., Chen Y.F., Zhu Z., Yao T., Koyama S., Shen M.Y. and Goto T., Optically pumped lasing of ZnO at room temperature, *Appl. Phys. Lett.,* **70,** 2230 **(1997)**
4. Srikant V., Valter S. and David R., Films on Sapphire: I, Effect of Substrate Orientation, *J. Am. Ceram. Soc.,* **78,** 1931 **(1995)**
5. Amlouk, Touhari F., Belgacem S., Kamoun N., Barjon D., Bennaceur R., Structural and Acoustic Properties of ZnO Thin Films Prepared by Spray. *Phys. Stat. Sol.* (A), **163,** 73–80 **(1997)**
6. Pauporte T. and Lincot D., Electrodeposition of Semiconductors for Optoelectronic Devices: Results on Zinc Oxide, *'Electrochim. Acta,* **45,** 3345 **(2000)**
7. Sahu D.R., Studies on the properties of sputter-deposited Ag-doped ZnO films, *Microelectron. J.*, **38,** 1252 **(2007)**
8. Morgan J.H. and Brodie D.E., The Preparation and Some Properties of Transparent Conducting ZnO for use in Solar Cells*, Can. J. Phys.* **60,** 1387 **(1982)**
9. Paraguay F., Estrada D.W., Acosta L.D.R. and Andrade N.E., M.Miki-Youshida, Growth, structure and optical characterization of high quality. ZnO thin films obtained by spray pyrolysis, *Thin Solid Films* **350,** 192 **(1999)**
10. Cui Y.G., Du G.T., Zhang Y.T., Zhu H.C. and Zhang B.L., *J. Cryst. Growth,* **282,** 389 **(2005)**
11. Heo Y.W., Norton D.P. and Pearton S.J., Zinc Oxide Bulk, Thin Films and nanostructures *.J. Appl. Phys.*, **98,** 073502 **(2006)**

12. Sun X.W. and Kwok H.S., *J. Appl. Phys*., **86,** 408 **(1999)**

13. Mridha S. and Basak D., .Effect of thickness on the structural, electrical and optical properties of ZnO films, *Mater. Res. Bull.,* **42,** 875 **(2007)**

14. Fahoume M., Maghfoul O., Aggour M., Hartiti B., Chraibi F. and Ennaoni A., Growth and characterization of ZnO thin films prepared by electrodeposition technique, *Sol. Energy Mater. Sol. Cells,* **90,** 1437–1444 **(2006)**

15. Bhargava R., (Ed.), Properties of Wide Bandgap II–VI, Semiconductors, London, **1997**

16. Yoshino K., Hata T., Kakeno T., Komaki H., Yoneta M., Akaki Y. and Ikari T., Electrical and optical characterization of n-type ZnO thin films, *Phys. Stat. Sol.* 626–630 **(2003)**

17. Harbeke G. (Ed.), Polycrystalline Semiconductors: Physical Properties and Applications, Berlin, **1985**

18. Vander A. Drift, *Philips Res. Rep.,* **22,** 267 **(1967)**

19. V. Assunc¸a˜o, E. Fortunato, A. Marques, A. Gonc¸ alves, I.Ferreira, H. A guas, R. Martins*, Thin Solid Films,* **442,** 121 **(2003)**

20. Gupta V. and Mansingh A., *J. Appl. Phys*., **80,** 1063–1073 **(1996)**

21. Cullity B.D., Elements of X-ray Diffraction, second edition, Addison-Wesley, **(1978)**

22. Minami T., Sato H., Takata S., Ogawa N. and Mouri T., *Jpn. J. Appl. Phys*., **3,** L1106–L1109 **(1992)**

23. Maniv S., Westwood W.D. and Colombini E., *J. Vac. Sci. Technol.,* **20,** 162 **(1982)**

24. Bilgin V., Kose S., Atay F. and Akyur I., *Mater. Chem. Phys.,* **94**, 103-108 **(2005)**

25. Seon J.B., Lee S., Kim J.M. and Jeong H.D., *Chem. Mater.,* **21,** 604-611 **(2009)**

26. Ortuño López M.B., Valenzuela-Jáuregui J.J., Sotelo-Lerma M., Mendoza- Galván A. and Ramirez-Bon R., Highly oriented CdS films deposited by an ammonia-free chemical bath method, *Thin Solid Films* **429**, 34- 39 **(2003)**

27. Hur T.B., Hwang Y.H., Kim H.K., Lee I.J., Strain effects in ZnO thin films and nanoparticles, *J. Appl. Phys.* **99,** 064308 **(2006)**

28. Patsalas P., Gravalidis C. and Logothetidis S., *J. Appl. Phys*., **96,** 6234– 6246 **(2004)**

29. Benger P.R., Chang K., Bhattacharya P., Singh J. and Bajaj K.K., Strain effects in ZnO thin films and nanoparticles, *Appl. Phys. Lett.* **53,** 684 **(1988)**

30. Gupta V. and Mansingh A., Influence of post deposition annealing on the structural and Optical Properties of sputtered Zinc Oxide Film, *J. Appl. Phys.* **80,** 1063–1073 **(1996)**

31. Chrysicopoulou P., Davazoglou D., Trapalis Chr. and Kordas G., Characterization of TiO2/Polyelectrolyte Thin Film Fabricated by a Layer-by-Layer Self-Assembly Method, *Thin Solid Films,* **323,** 188 **(1998)**

32. Mayadas A.F. and Shatzkes M., Electrical-resistivity model for polycrystalline films: the case of arbitrary reflection at external surfaces, *Phys Rev B,***1,** 1382-9 **(1970)**